J. Agr. Sci. Tech. (2019) Vol. 21(2): 309-322

Prediction and Optimization of Fish Biodiesel Characteristics Using Permittivity Properties

M. Zarein[1], M. H. Khoshtaghaza[1*], B. Ghobadian[1], and H. Ameri Mahabadi[2]

ABSTRACT

The purpose of this research was to predict and optimize the fish biodiesel characteristics using its permittivity properties. The parameters of biodiesel permittivity properties such as έ, dielectric constant, and ε″, loss factor at microwave frequencies of 434, 915, and 2,450 MHz, were used as input variables. The fish biodiesel characteristics, as Fatty Acid Methyl Ester (FAME) content and flash point at three different levels of reaction time 3, 9, and 27 min and catalyst concentrations 1, 1.5, and 2% w w_{oil}^{-1}, were selected as output parameters for the models. Linear Regression (LR), the Multi-Layer Perceptron (MLP), and the Radial Basis Function (RBF) as the methods of Artificial Neural Networks (ANN), and the response surface methodology were compared for prediction and optimization of FAME content and flash point. A comparison of the results showed that the RBF recorded higher coefficient of determination at frequency of 2,450 MHz as 0.999 and 0.988 and lower root mean square error as 0.009 and 0.023 for FAME content and flash point, respectively. The optimum condition was obtained using RSM by FAME content of 89.88% and flash point of 152.7°C with desirability of 0.998.

Keywords: Artificial neural network, Fatty acid methyl ester content, Flash point, Optimum condition, Response surface methodology.

INTRODUCTION

Waste Fish Oil (WFO) is produced in large quantity by fish-processing industry as a by-product in Iran. This by-product has similar calorific value to petroleum distillates and is a renewable energy source (Yahyaee *et al*., 2013). Biodiesel is defined as a fuel that contains mono-alkyl esters of long chain fatty acids (Ghobadian *et al*., 2008). One of the advantages of using biodiesel fuel is the significant reduction in emissions such as CO and HC. Therefore, biodiesel produced from oilseed crops can be used as fuel that is required by diesel engines (Ghazali *et al*., 2015: Abedin *et al*., 2014).

Biodiesel has been produced globally from several products such as waste fish oil (García-Moreno *et al*., 2014), palm oil (Tan *et al*., 2011), sunflower oil (Yin *et al*., 2012), vegetable oil (Kouzu and Hidaka, 2012), waste cooking oil (Talebian-Kiakalaieh *et al*., 2013) and rapeseed oil (Duren *et al*., 2015). Since Free Fatty Acid (FFA) content is a critical parameter in the conversion of fish oils to methyl esters, the performance of a Fourier Transform InfraRed (FTIR) spectroscopic method was assessed as an alternative to the conventional AOCS titrimetric method (Alberta *et al*., 2009). The properties of the triglyceride and the biodiesel fuel are determined by the amounts of each fatty acid present in their molecules. Transesterification does not alter the fatty acid composition of the feedstock and this composition plays an important role in some critical parameters of the biodiesel, as viscosity and flash point properties (Mejia *et al*., 2013; Ramos *et al*., 2009). Incorporating ultrasonic energy into traditional transesterification reactions can emulsify the reactants to reduce the requirement of catalyst amount, methanol-to-

[1] Department of Mechanical and Biosystems Engineering, Tarbiat Modares University, Tehran, Islamic Republic of Iran.
[2] Department of Electrical Engineering, University of Malaya (UM), Kuala Lumpur, Malaysia.
[*]Corresponding author; e-mail: khoshtag@modares.ac.ir

[DOR: 20.1001.1.16807073.2019.21.2.14.5]

oil ratio, reaction time and reaction temperature (Parkar *et al*., 2012; Santos *et al*., 2009). In biodiesel production using ultrasonic, the maximum reaction time to reach the maximum conversion rate for castor, palm, and fish oil were obtained as 9, 63, and 27 minutes, respectively (Maghami *et al*., 2015).

Dielectric spectroscopy has been successfully used for production and characterization of biodiesel (Sorichetti and Romano, 2005). It is used to characterize feedstocks from different origins (Corach *et al*., 2014), to detect alcohol in the light phase after the completion of the transesterification process (Ramos *et al*., 2009), during the purification process and in the final product (Gonzalez *et al*., 2008), and also for the characterization of FAME (Corach *et al*., 2012). Based on geographic limitations and oil prices, biodiesel can be produced from a variety of feedstocks and different technologies can be applied for biodiesel production (Oliveira *et al*., 2008; Balabin *et al*., 2010). Consequently, the final product can have different properties, so, the quality control of biodiesel is very important. The EN 14214 mandates 25 parameters that have to be analyzed to certify biodiesel quality and these analyses are expensive and time consuming (Flores *et al*., 2012; Silva *et al*., 2017). Measurements of dielectric properties at microwave frequencies offer several advantages for characterization (Romano and Sorichetti, 2011). Particularly in the microwave range, the technique is fast, accurate, simple, cheap, and non-destructive (Liptak, 2003).

Artificial Neural Network (ANN) and Response Surface Methodology (RSM) have been widely applied for modeling and optimization of biodiesel synthesis from various feedstocks using different methods such as classical base catalyzed transesterification (Stamenkovic *et al*., 2015; Rajkovic *et al*., 2013), heterogeneous base catalyzed transesterification (Betiku and Ajala, 2014), ultrasound assisted base catalyzed transesterification (Moorthi *et al*., 2015), infrared irradiation assisted esterification (Chakraborty and Sahu, 2014). Different ANN models based on multi-layer feed forward, radial base, generalized regression, and recurrent network were developed for predicting the Cetane Number (CN) of biodiesel fuel (Ramadhas *et al*., 2006). The biodiesel production from rapeseed soap stock and methanol in the presence of the *candida rugosa* lipase immobilized on chitosan was analyzed. Using ANN showed desirable correspondence between predicted and experimental values of the FAME yield (Ying *et al*., 2009).

The aim of this study was, therefore, to develop ANN models to predict the Fatty Acid Methyl Ester (FAME) content and flash point during biodiesel production using permittivity properties of biodiesel as the ANN inputs and optimize the conditions of these characteristics by RSM.

MATERIALS AND METHODS

Waste Fish Oil (WFO) was purchased from fishmeal plant in Semnan, Iran. WFO properties like acid value, density, kinematic viscosity, flash point, Free Fatty Acid (FFA) content, color and mean molecular weight were measured (Table 1). All chemicals, such as methanol, KOH, H_2SO_4 with purity of 99.99%, were analytical grade and purchased from Merck (Germany). The ultrasonic processor UP400S (400W, 24 kHz) with probe diameter of 40 mm and probe length of 100 mm was made by Hielscher (Germany).

Experimental Procedure

Esterification was applied to reduce FFA content. Methanol and waste fish oil were transmitted to two-layer 250 mL glass reactor which was equipped with temperature control (±1°C) and condenser. For the temperature control, external heating was applied with an accuracy of ±1°C. Experiments were carried out in the temperature range of 40-60°C. Sulfuric acid

[DOR: 20.1001.1.16807073.2019.21.2.14.5]

Table 1. Chemical and physical properties of the used WFO.

Property	Units	Measured value
Acid value	mg KOH g^{-1} oil	9.98±0.02
Density (@15°C)	g cm^{-3}	0.912±0.007
Kinematic viscosity (@25°C)	mm^2 s^{-1}	44.551±2.685
Flash point, Closed cup	°C	196±1
FFA content	%	5.47±0.01
Color	-	Dark brown
Mean molecular weight of WFO	g mol^{-1}	903

(1% wt wt^{-1}) was used as catalyst and reaction continued for 1 h to reduce FFA content. Transesterification is a reversible reaction that requires more Methanol Ratio (MR) than the stoichiometric values to reach the higher product yields (Vicente *et al*., 2007; Leevijit *et al*., 2008). The optimum condition of biodiesel production is related to the type and amount of catalysts and oils (Zheng *et al*., 2006). For acid catalysis reactions, always higher ratios were suggested with longer reaction times. After FFA conent reduction, the reactor content was removed for separating funnel and allowed to separate layers methanol-reach phase and esterified oil. Homogenous base catalysts are used widely for the biodiesel production. These catalysts have more conversion when compared to the acid, enzyme, or base heterogeneous catalysts. For this reason, potassium hydroxide as a homogeneous catalyst was used in this work for the biodiesel production from waste fish oil. Catalyst type and loading amount are the main parameters that affect the biodiesel production. Lower catalyst loading caused minor conversion and higher loading caused side reactions like saponification in transesterification process. The properties of the produced biodiesel in comparison with the ASTM D6751 standard are described in Table 2. FAME content and flash point at different catalyst concentration of 1, 1.5, and 2% w w_{oil}^{-1} and reaction time of 3, 9 and 27 min were measured.

Biodiesel Characteristics Measurement

The fatty acid compositions of the biodiesel and waste oil were analyzed using a Gas Chromatography (GC) analyzer (Claus 580 GC model, Perkin Elmer Co., USA). The inert temperature of GC was 250°C and helium gas (purity 99.999%) with 1 mL min^{-1} flow used as mobile phase. Nonadecanoic acid (C19:0) was used as a standard sample which was measured and added to each sample before GC analysis (Figure 1).

The FAME content of each sample was calculated according to equation (1):

$$FAME\ content\ (\%) = \frac{[\sum A] - A_i}{A_i} \times \frac{m_i}{M} \times 100 \quad (1)$$

Where, *i* is standard sample and A_i and A are the peak Areas of standard and total sample in GC reports, respectively. M is the weight of sample and m_i is the weight of standard in the sample. Weight of product was estimated after separation of glycerin phase and removal of impurities by washing and drying of biodiesel phase in each experiment. The flash point test was carried out by FLPH (CCCFP) Continuously Close Cup (Grabner, Austria) according to ASTM D93. For measuring acid number and Free Fatty Acid (FFA) content of WFO, 1 g of waste oil was dissolved in 10 mL 2-propanol and then titrated by KOH 0.1M (5.61 mg KOH in 1 mL ethanol) in the presence of phenolphthalein as indicator (Maghami *et al*., 2015). Acid number is mg KOH which is used for titration of 1 g oil and FFA content was calculated by Equation (2).

$$FFA\% = \frac{V.C.M}{10.m} \quad (2)$$

Where, V is KOH solution Volume (mL), C is solution molarity (0.1 mol L^{-1}), M is WFO Molecular weight (g mol^{-1}) and m is WFO weight (g).

[DOR: 20.1001.1.16807073.2019.21.2.14.5]

(a)

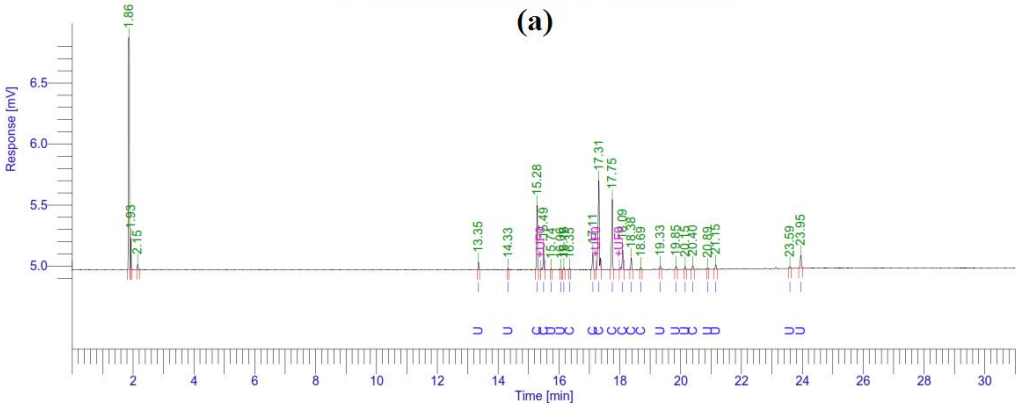

(b)

Figure 1. (a) Gas Chromatography (GC) analyzer and (b) The yields of WFO compounds according to the carbon chain by GC.

Permittivity Measurement

The permittivity properties of a substance may be described in the frequency domain by the complex permittivity, ε. The real part (dielectric constant), $\acute{\varepsilon}$, represents electrical polarization and the imaginary part (loss factor), ε'' is related to energy dissipation as the following equation (Corach *et al*., 2015):

$$\varepsilon = \acute{\varepsilon} - j\varepsilon'' \quad (3)$$

Permittivity properties of the mixtures were determined using an Agilent ENA series E5071C Network Analyzer with Agilent 85070E dielectric probe kit (Agilent Technologies, Inc. Santa Carla, CA) using coaxial line method at frequency of 434, 915 and 2,450 MHz according to ISM standard. Frequency values were selected based on the limits of measurement system, because of Agilent 85070E dielectric probe kit is suitable for frequencies above 200 MHz (Muley and Boldor, 2013). The network analyzer was controlled by Agilent 85070E dielectric kit software and calibrated using the 3-point method (short-circuit, air and water at 25°C).

Linear Regression Model

Regression analysis is a statistical technique for examining and modeling the association between variables. It is a widely used statistical technique that operates by building mathematical equations relating the response (variable) to set the predictors or independent variables. Linear Regression (LR) was used to model the values of a dependent variable based on a linear relationship with one or more predictors. A LR model assumes that there is a linear relationship (denoted by a straight line) between the dependent variables and the independent variables (Rodriguez *et al*.,

[DOR: 20.1001.1.16807073.2019.21.2.14.5]

2014). The LR model is often formulated as Equation (4):

$$y = b_0 + b_1 x_1 + \cdots + b_n x_n + e \quad (4)$$

Where, y is the value of the dependent variable, x_n is the predictor variable, b_n is the coefficient value, and e is the observed error (uncontrolled factors and experimental error). The model parameters (b_j) were estimated using a regression model.

Artificial Neural Networks (ANN) Models

Neural networks may be used as a direct substitute for auto correlation, multivariable regression, linear regression, trigonometric and other statistical analysis and techniques (Singh *et al*., 2003). Multi Layer Perceptron (MLP) and Radial Basis Function (RBF) are two of the most widely used neural network architecture in literature for classification or regression problems (Cohen and Intrator, 2003). Both types of neural network structures are good in pattern classification problems. The output of a MLP is produced by linear combinations of the outputs of hidden layer nodes in which every neuron maps a weighted average of the inputs through a sigmoid function. In one hidden layer RBF network hidden nodes map distances between input vectors and center vectors to outputs through a nonlinear kernel or radial function (Balabin *et al*., 2011). In this study, the two different architectures of ANN (MLP and RBF) were also used to estimate the FAME content and flash point. All data were first normalized and divided into three data set such as training (70% of all data), test (15% of all data) and verification (15% of all data). The STATISTICA12 software was used in neural network analysis having a three-layer feed-forward network that consists of an input layer (2 neurons), one hidden layers (2 neurons for MLP, 15 neurons for RBF) and two output layer (Figure 2). Neuron numbers in hidden layers were selected from a series of trial runs of the networks having 1 neuron to 20 neurons in order to obtain the neuron number in the network having minimum error. Variable learning rate with momentum (trainLm) as networks training function and tangent sigmoid (tansig) was used as an activation (transfer) function for all layers (Yilmaz and Kaynar, 2011).

Response Surface Methodology (RSM)

Response Surface Methodology (RSM) has an important application in the design, development, and formulation of new products, as well as in the improvement of existing product design. It defines the effect of the independent variables, alone or in combination, on processes. In addition, to analyze the effects of the independent variables, this experimental methodology generates a mathematical model which describes the chemical or biochemical processes (Halim *et al*., 2009). In order to obtain the optimum value, Equation (5) is used:

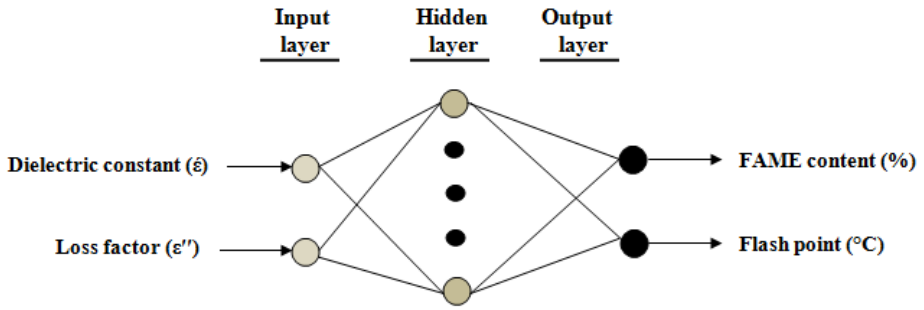

Figure 2. MLP and RBF neural network structure used in the study.

[DOR: 20.1001.1.16807073.2019.21.2.14.5]

$$Y_i = \beta_0 + \sum \beta_i X_i + \sum \beta_{ij} X_i X_j + \sum \beta_{jj} X_i^2 + \varepsilon \quad (5)$$

Where, $ß_0$, $ß_i$, $ß_{ij}$, $ß_{jj}$ are regression coefficients for intercept, linear, interaction, and quadratic coefficients, respectively, while Xi and Xj are coded independent variables and ε is the error. In the present study, Box-Behnken design with 3 central points was used.

The validation and performance of the LR, MLP, RBF, and RSM models were compared using R^2, *MAPE*, and *RMSE* as follows, equations (6-8) (Amid and Mesri Gundoshmian, 2016):

$$R^2 = 1 - \left(\frac{\sum_{i=1}^{n}(z_i - \acute{z})^2}{\sum_{i=1}^{n} z_i^2}\right) \quad (6)$$

$$\text{MAPE} = \frac{1}{N}\sum_{i=1}^{N}\left|\frac{z_i - \acute{z}}{z_i}\right| \times 100 \quad (7)$$

$$RMSE = \sqrt{\frac{\sum_{i=1}^{n}(z_i - \acute{z})^2}{N}} \quad (8)$$

Where, z_i is the measured value, z' is the predicted value, and N is the total Number of observations (Yilmaz and Yuksek, 2009; Garg *et al*., 2015). R^2 is a descriptive measure between zero and one and indicates the ability of a parameter to predict another parameter. The highest value for *MAPE* (100) and the lowest value for *RMSE* (0) denote the highest values for model performance. *MAPE* usually gives accuracy as a percentage and a low percentage for this parameter denotes good performance of the model (Khoshnevisan *et al*., 2014). This research was carried out using SPSS 24.0, STATISTICA12 and Design Expert 7 software.

RESULTS AND DISCUSSION

Evaluation of Linear Regression Model

In this paper, FAME content and flash point are assumed to be a function of dielectric constant (έ) and loss factor (ε″) at three different frequencies. The obtained LR models for prediction of FAME content and flash point are presented in Table 3.

R^2 was used to ascertain the predictive performance of the model for the measured and predicted values. For example, it shows that R^2 for the relationships between the measured and predicted values obtained at frequency of 2,450 MHz from the LR models for FAME content and flash point demonstrate suitable correlation (Figure 3).

Evaluation of MLP Model

Input parameters of dielectric constant and loss factor were selected as input variables and FAME content and flash point were chosen as model outputs. The results showed that the best model was that with one input layer and two input variables, one hidden layer with 18 neurons, and one output layer and one output variable (2–18–1 structure). Cross-correlation of the predicted and target values at frequency of 2,450 MHz (Figure 4) indicated that the ANN MLP model was most acceptable. The R^2, *RMSE* and *MAPE* for the output variables are shown in Table 4.

Evaluation of RBF Model

The performance of RBF networks for estimated performance characteristics modeling used a single-layer neural network. Input directly entered the hidden layer cells and the output of the hidden layer cells multiplied by the weights entered a collector as the output of the neural network. Input-output data for network training were the same as that used to generalize the MLP network. The error value was zero and the network attained this error with 40 cells in the hidden layer. Figure 5 shows scatter plots of the

Table 3. LR models for prediction of FAME content and flash point.

Frequency (MHz)	FAME Content (%)	R^2	Flash Point (°C)	R^2
434	*FC= 41.7έ+50.6ε″-110.6*	0.995	*FP= -19.8έ-34.5ε″+257.8*	0.933
915	*FC= 34.9έ+52.6ε″-86.5*	0.968	*FP= -16.9έ-35.3ε″+246.7*	0.920
2450	*FC= 43.6έ+51.8ε″-111.8*	0.994	*FP= -21.1έ-36.2ε″+264.5*	0.941

[DOR: 20.1001.1.16807073.2019.21.2.14.5]

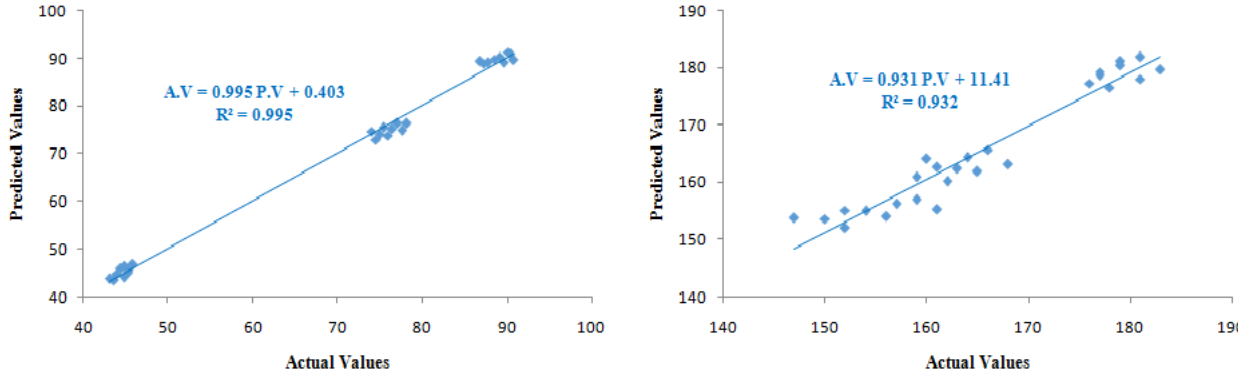

Figure 3. Cross-correlation of predicted and actual values of (a) FAME content and (b) Flash point for LR model at frequency of 2,450 MHz.

predicted FAME content and flash point based on the actual values.

R^2, *RMSE* and *MAPE* are shown in Table 4. The results show that the RBF model had high acceptability for prediction of output parameters at frequency of 2,450 MHz. The MLP, RBF, and RSM were applied for prediction of biodiesel production from crude mahua (*Madhuca indica*) oil and compared the results with those from a Multiple Regression (MR) model (Sarve *et al*., 2015). Comparison of factors indicated that RBF had the lowest *MAPE* and *RMSE* and the highest R^2. It can be concluded that the RBF performed much better than MLP and MR for predicting the FAME content and flash point.

Comparison between the Models

This study was developed and compared LR and ANN (MLP-RBF) methods for determining FAME content and flash point. The results of simple regression analysis showed a statistically suitable relationship between the output and input characteristics. The prediction models were developed with two inputs and outputs and the networks were evaluated for each output separately. The results of prediction of FAME content and flash point indicated that the equations obtained from the ANN-MLP model

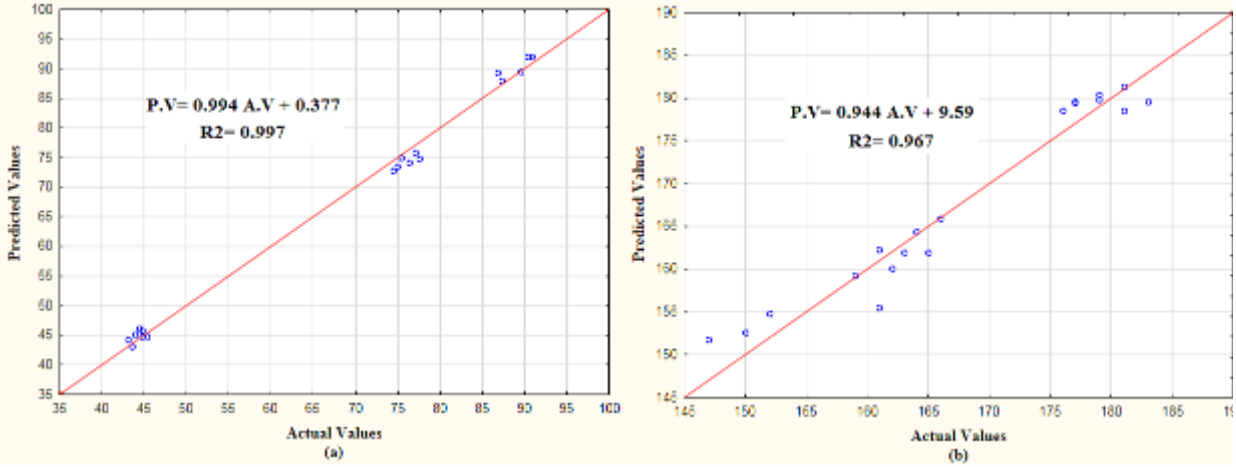

Figure 4. Cross-correlation of predicted and actual values of (a) FAME content and (b) Flash point for ANN (MLP) model at frequency of 2,450 MHz.

[DOR: 20.1001.1.16807073.2019.21.2.14.5]

Table 4. Performance indices (R^2, RMSE and MAPE) for models at various frequencies.

Frequency (MHz)	Model	FAME content			Flash point		
		R^2	*RMSE*	*MAPE* (%)	R^2	*RMSE*	*MAPE* (%)
434	LR	0.995	0.011	1.603	0.933	0.039	1.387
	ANN-MLP	0.997	0.008	1.459	0.969	0.014	1.168
	ANN-RBF	0.998	0.005	1.261	0.986	0.011	1.106
915	LR	0.968	0.027	3.712	0.920	0.042	1.454
	ANN-MLP	0.996	0.015	1.381	0.989	0.021	1.292
	ANN-RBF	0.998	0.008	1.137	0.993	0.014	1.137
2450	LR	0.994	0.012	9.801	0.941	0.036	1.967
	ANN-MLP	0.997	0.009	1.439	0.967	0.023	1.472
	ANN-RBF	0.999	0.003	1.183	0.988	0.009	1.069

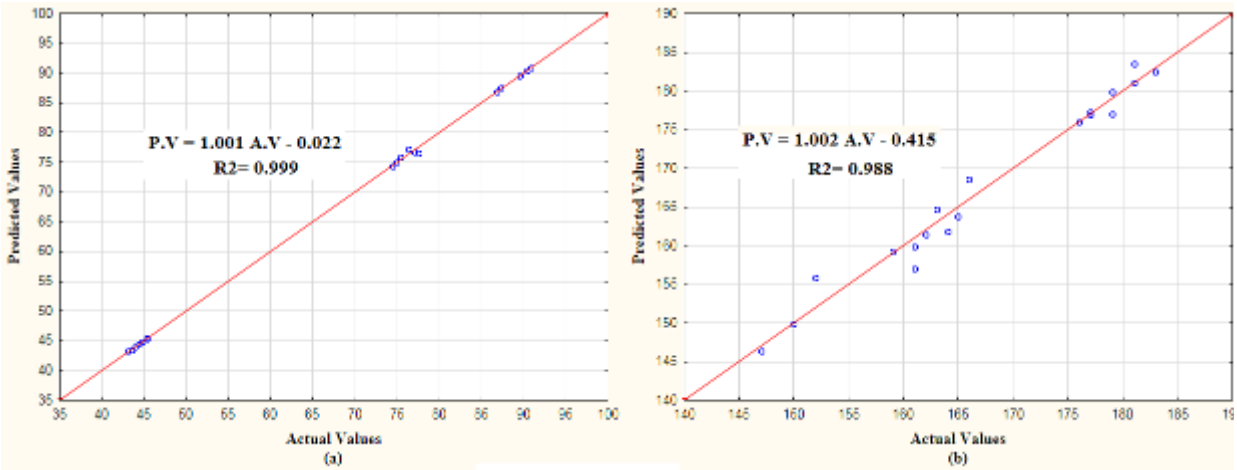

Figure 5. Cross-correlation of predicted and actual values of (a) FAME content and (b) Flash point for ANN (RBF) model at frequency of 2,450 MHz.

provided more suitable and reliable prediction than LR model. Besides, the RBF with two inputs and one output exhibited greater reliability of prediction than the LR and MLP models. Also, the values for R^2, *RMSE* and *MAPE* indicated that the prediction performance of the ANN-RBF model was better than LR and ANN-MLP (Table 4).

Optimization Using Response Surface Method (RSM)

In this paper, Box-Behnken design was employed to develop a relationship between biodiesel characteristics (FAME content and flash point) and independent variables (dielectric constant and loss factor) in order to maximize the FAME content and minimize the flash point. The FAME content and flash point varied from 43.1 to 90.8% and 147 to 183°C, respectively. The application of the advanced multiple regression analysis was employed to obtain the polynomial equation at frequency of 2,450 MHz. The equations of the significant terms obtained from the model in its coded form are as follows (Equations 9-10):

$$FAME\ content = -312.83 + 143.78\ \acute{\varepsilon} + 129.19\ \varepsilon'' - 19.27\ \acute{\varepsilon}\varepsilon'' - 12.76\ \acute{\varepsilon}^2 - 8.92\ \varepsilon''^2 \quad (R^2 = 0.998) \quad (9)$$

$$Flash\ Point = +245.32 - 27.46\ \acute{\varepsilon} + 48.65\ \varepsilon'' - 22.03\ \acute{\varepsilon}\varepsilon'' + 3.25\ \acute{\varepsilon}^2 - 7.03\ \varepsilon''^2 \quad (R^2 = 0.948) \quad (10)$$

From the above equations, the coefficient with one factor signifies the effect in an individual form, while the coefficient which has two factors and second order form signifies the interaction between them and their fourth route effect. The suffix symbols positive or negative (+/-) signify

[DOR: 20.1001.1.16807073.2019.21.2.14.5]

the synergy and antagonistic effects, where the positive stands for synergistic effect and the negative stands for antagonistic effect (Joshi *et al*., 2008). Then, the model was analyzed by Analysis Of Variance (ANOVA) for obtaining the fitness of the model employing least square method. The effective statistical technique which bifurcates into individual roots which allows user to understand the sum of all the variation of the data in the model with specific sources of variation is ANOVA (Yatish *et al*., 2016). Thus, the obtained models variations are presented in Table 5.

Figure 6 shows an acceptable correlation between the predicted and experimental values of FAME content and flash point at frequency of 2,450 MHz, with a high value of coefficient of determination (R^2) 0.998 and 0.948, respectively.

The surface plots in three dimensions represent the graphical interface about the regression equation of reaction variables. Figure 7 represents the surface plots of biodiesel characteristics. Plots "a" and "b" illustrate the interaction between two independent variables on the dependent parameter. The plots are drawn with the aid of the regression equation and represent the interactions of each independent variable on the response variables. Plot a represents the significant interaction between dielectric constant (έ) and loss factor (ε″), the variation in the FAME content is depicted well in the plot, i.e. the FAME content at first increases significantly by increasing both dielectric constant and loss factor. Plot "b" shows the nature of dielectric constant and loss factor on the flash point. Here, it could find a proportional increase in the flash point as the dielectric constant decreases, whereas a slight increase can be seen when the loss factor is decreased too.

Finally, to reach the optimization of biodiesel characteristics such that to maximize the FAME content and minimize the flash point values at frequency of 2,450 MHz, the conditions were suggested as in Table 6.

The optimum condition with desirability of 0.998 was obtained as dielectric constant of 3.72 and loss factor of 0.89 for FAME content of 89.88% and flash point of 152.7°C.

CONCLUSIONS

Prediction of biodiesel characteristics based on its permittivity properties can help estimate the quality and simulate the production process. Production systems assess the conditions during processing and is complex because the data is generally inconsistent. This research work was applied to the LR, MLP and RBF models which were developed using these initial conditions to predict FAME content and flash point. The results showed for FAME content and flash point, R2 values at frequency of 2450 MHz were calculated as 0.994 and 0.941 for LR model, 0.997 and 0.967 for MLP of ANN model, 0.999 and 0.988 for RBF of ANN model, respectively. The RBF model was exhibited high performance rather than the MLP and LR models for prediction the output data. The use of the RBF model may provide new

Table 5. Experimental process obtained for biodiesel characteristics at frequency of 2,450 MHz.

Run	Dielectric constant (έ)	Loss factor (ε″)	FAME content (%)		Flash point (°C)	
			Predicted	Obtained	Predicted	Obtained
1	3.91	0.68	86.76	87.3	158.90	159
2	3.84	0.75	87.51	87.7	156.89	157
3	3.77	0.82	88.23	86.8	155.06	161
4	3.82	0.8	88.97	89.1	154.95	154
5	3.74	0.85	88.54	89.6	154.33	152
6	3.68	0.91	89.13	88.6	152.96	156
7	3.71	0.92	90.50	90.4	151.80	150
8	3.65	0.97	90.67	90.8	150.97	147
9	3.57	1.02	90.17	90.1	150.80	152

[DOR: 20.1001.1.16807073.2019.21.2.14.5]

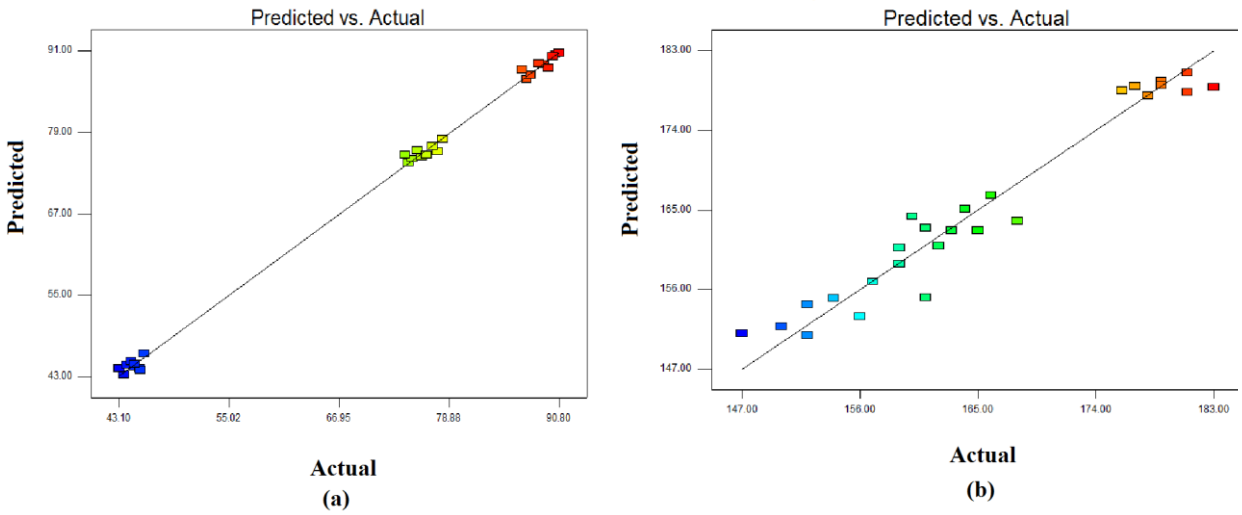

Figure 6. Actual values vs. predicted values of (a) FAME content and (b) Flash point at frequency of 2,450 MHz.

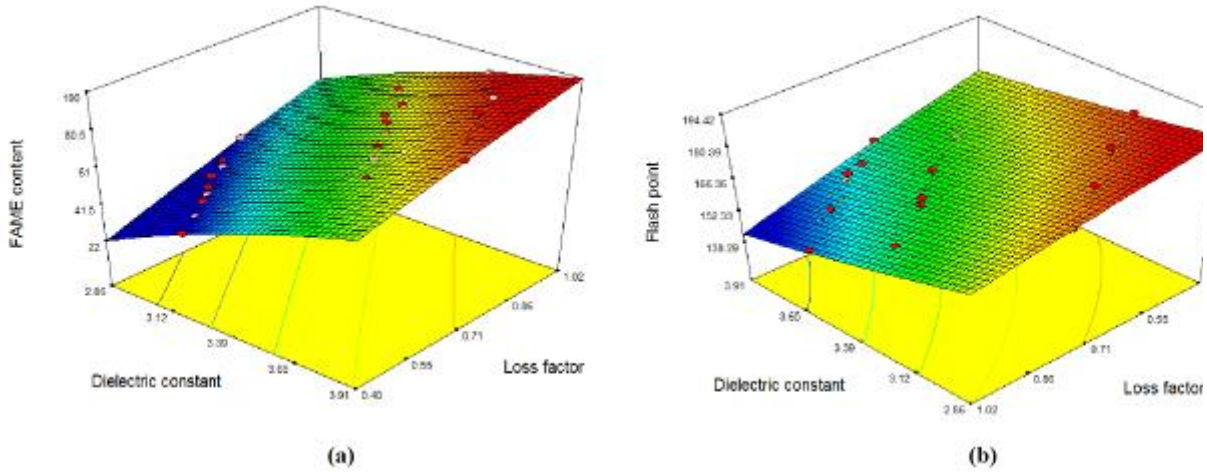

Figure 7. Surface plots of (a) FAME content and (b) Flash point at frequency of 2,450 MHz.

Table 6. Suggested conditions to reach optimum biodiesel characteristics.

Number	Dielectric constant (έ)	Loss factor (ε″)	FAME content (%)	Flash point (°C)	Desirability
1	**3.72**	**0.89**	**89.88**	**152.7**	**0.998**
2	3.72	0.88	89.52	152.9	0.997
3	3.65	0.91	88.19	153.6	0.995
4	3.67	0.89	88.01	154.1	0.991
5	3.55	0.96	86.99	153.9	0.986
6	3.61	0.87	84.94	156.5	0.983
7	3.72	0.78	84.88	157.9	0.979
8	3.82	0.64	82.45	162.1	0.978

[DOR: 20.1001.1.16807073.2019.21.2.14.5]

approaches and methodologies, and minimize potential inconsistency of correlation. A comparison of the RBF network and MLP models indicates that RBF can be used efficiently to model and predict output data based on input parameters with similar accuracy. The optimum condition was obtained using response surface methodology as dielectric constant of 3.72, loss factor of 0.89 at frequency of 2450 MHz lead to reach the FAME content of 89.88% and flash point of 152.7°C with desirability of 0.998.

Nomenclature

A_i, A	Peak area of standard and total sample (V sμ)
ANN	Artificial Neural Network
b_j	Model parameter
b_n	Coefficient value
C	Solution molarity (0.1 mol L^{-1})
CN	Cetane Number
e	Observed error
f	Frequency (MHz)
FAME	Free Acid Methyl Ester
FFA	Free Fatty Acid
GC	Gas Chromatography
LR	Linear Regression
M	Weight of sample (mg)
m	WFO weight (g)
MAPE	Mean Absolute Percentage Error
m_i	Weight of standard in the sample (mg)
MLP	Multi Layer Perceptron
MR	Methanol Ratio
N	Total number of observations
RBF	Radial Basis Function
RMSE	Root Mean Square Error
RSM	Response Surface Method
V	KOH solution volume (ml)
WFO	Waste Fish Oil
X_i , X_j	Coded independent variables
x_n	Predictor variable
Z_i , Z'	Measured and predicted value
β	Regression coefficient
ε	Complex dielectric
$\acute{\varepsilon}$	Dielectric constant
ε''	Loss factor

REFERENCES

1. Abedin, M. Masjuki, H. H. Kalam, M. A. Sanjid, A. Ashraful Rahman, S. M. and Rizwanul Fattah, I. M. 2014. Performance, Emissions, and Heat Losses of Palm and Jatropha Biodiesel Blends in a Diesel Engine. *Ind. Crops Prod.*, **59:** 96-104.
2. Alberta, N. A., Frederik, R., Voort, V. D. and Benjamin, K. 2009. FTIR Determination of Free Fatty Acids in Fish Oils Intended for Biodiesel Production. *Ind. Crops Prod.*, **59:** 96-104.
3. Amid, S. and Mesri Gundoshmian, T. 2016. Prediction of Output Energy Based on Different Energy Inputs on Broiler Production Using Application of Adaptive Neural-Fuzzy Inference System. *Agri. Sci. Dev.*, **5:** 14-21.
4. Balabin, R. M., Safieva, R. Z. and Lomakina, E. I. 2010. Gasoline Classification Using Near Infrared (NIR) Spectroscopy Data: Comparison of Multivariate Techniques. *Analy. Chimi. Acta*, **671:** 27-35.
5. Balabin, R. M., Lomakina, E. I. and Safieva, R. Z**.** 2011. Neural Network (ANN) Approach to Biodiesel Analysis: Analysis of Biodiesel Density, Kinematic Viscosity, Methanol and Water Contents using Near Infrared (NIR) Spectroscopy. *Fuel*, **90:** 2007-2015.
6. Betiku, E. and Ajala, S. O. 2014. Modeling and Optimization of Thevetia Peruviana (Yellow Oleander) Oil Biodiesel Synthesis via Musa Paradisiacal (Plantain) Peels as Heterogeneous Base Catalyst: A Case of Artificial Neural Network vs. Response Surface Methodology. *Ind. Crops Prod.*, **53:** 314–322.
7. Chakraborty, R. and Sahu, H. 2014. Intensification of Biodiesel Production from Waste Goat Tallow using Infrared Radiation: Process Evaluation through Response Surface Methodology and Artificial Neural Network. *Appl. Ener.*, **114:** 827–836.
8. Cohen, S. and Intrator, N. 2003. A Study of Ensemble of Hybrid Networks with Strong Regularization. *Multi. Classi. Sys.*, **4:** 227–235.
9. Corach, J., Sorichetti, P. A. and Romano, S.D. 2012. Electrical Properties of Mixtures of Fatty Acid Methyl Esters from Different Vegetable Oils. *Int. J. Hydro. Ener.*, 37: 14735–14739.
10. Corach, J., Sorichetti, P. A. and Romano, S. D. 2014. Electrical Properties of Vegetable Oils between 20 Hz and 2 MHz. *Int. J. Hydro. Ener.*, **39:** 8754–8758.

[DOR: 20.1001.1.16807073.2019.21.2.14.5]

11. Corach, J., Sorichetti, P. A. and Romano, S. D. 2015. Electrical and Ultrasonic Properties of Vegetable Oils and Biodiesel. *Fuel*, **139**: 466–471.
12. Dawson, C. W. and Wilby, R. 1998. An Artificial Neural Network Approach to Rainfall-Runoff Modeling. *Hydrolo. Sci. J.*, **43:** 47–66.
13. Deh Kiani, M. K., Ghobadian, B., Tavakoli, T., Nikbakht, A. M. and Najafi, G. 2010. Application of Artificial Neural Networks for the Prediction of Performance and Exhaust Emissions in SI Engine using Ethanol-Gasoline Blends. *Energy*, **35:** 65–69.
14. Duren, I. V., Voinov, A., Arodudu, O. and Firrisa, M. T. 2015. Where to Produce Rapeseed Biodiesel and Why? Mapping European Rapeseed Energy Efficiency. *Renew. Ener*., **74:** 49-59.
15. Flores, I. S., Godinho, M. S., De Oliveira, A. E., Alcantara, G. B., Monteiro, M. R., Menezes, S. M. C. and Lião, L. M. 2012. Discrimination of Biodiesel Blends with 1H NMR Spectroscopy and Principal Component Analyses. *Fuel*, **99:** 40-44.
16. Foody, G. M. 2004. Supervised Image Classification by MLP and RBF Neural Networks with and without an Exhaustively Defined Set of Classes. *Int. J. of Remote Sens.*, **25:** 3091–3104.
17. García-Moreno, P. J., Khanum, M., Guadix, A. and Guadix, E. M. 2014. Optimization of Biodiesel Production from Waste Fish Oil. *Renew. Ener.*, **68:** 618-624.
18. Garg, A., Vijayaraghavan, V., Tai, K., Singru, P. M., Jain, V. and Krishnakumar, N. 2015. Model Development Based on Evolutionary Framework for Condition Monitoring of a late Machine. *Measurement*, **73:** 95–110.
19. Ghazali, W. N. M. W. Mamat, R. Masjuki, H. H. and Najafi, G. 2015. Effects of Biodiesel from Different Feedstocks on Engine Performance and Emissions: A Review. *Renew. Sustain. Ener. Rev.*, **51:** 585-602.
20. Ghobadian, B., Tavakoli Hashjin, T. and Rahimi, H. 2008. Production of Bioethanol and Sunflower Methyl Ester and Investigation of Fuel Blend Properties. *J. Agri. Sci. Tech.*, **10:** 225-232
21. Gonzalez, P. L., Sorichetti, P. A. and Romano, S. D. 2008. Electric Properties of Biodiesel in the Range from 20 Hz to 20 MHz. Comparison with Diesel Fossil Fuel. *Int. J. Hydro. Ener.*, **33:** 3531–3537.
22. Halim, S. F. A., Kamaruddin, A. H. and Fernando, W. J. N. 2009. Continuous Biosynthesis of Biodiesel from Waste Cooking Palm Oil in a Packed Bed Reactor: Optimization using Response Surface Methodology (RSM) and Mass Transfer Studies. *Biores. Tech.*, **100:** 710-716.
23. Joshi, A., Pund, S., Nivsarkar, M., Vasu, K. and Shishoo, C. 2008. Dissolution Test for Site-Specific Release Ionized Pellets in USP Apparatus 3 (Reciprocating Cylinder): Optimization using Response Surface Methodology. *Eur. J. Pharm. Biopharm.*, **69:** 769–775.
24. Khoshnevisan, B., Rafiee, S., Omid, M. and Mousazadeh, H. 2014. Prediction of Potato Yield Based on Energy Inputs Using Multi-Layer Adaptive Neuro-Fuzzy Inference System. *Measurement*, **47:** 521–530.
25. Kouzu, M. and Hidaka, J. S. 2012. Transesterification of Vegetable Oil into Biodiesel Catalyzed by CaO: A Review. *Fuel*, **93:** 1-12.
26. Leevijit, T., Tongurai, C., Prateepchaikul, G. and Wisutmethangoon, W. 2008. Performance Test of a 6-Stage Continuous Reactor for Palm Methyl Ester Production. *Bioresour. Tech.*, **99:** 214-221.
27. Liptak, B. G. 2003. *Instrument Engineers 'Handbook: Process Measurement and Analysis.* 4th Edition, Section 8.52, Chapter 8, Vol. I, CRC Press.
28. Maghami, M., Sadrameli, S. M. and Ghobadian, B. 2015. Production of Biodiesel from Fishmeal Plant Waste Oil using Ultrasonic and Conventional Methods. *App. Ther. Eng*., **75:** 575-579.
29. Mejia, J. D., Salgado, N. and Orrego, C**. E.** 2013. Effect of Blends of Diesel and Palm-Castor Biodiesels on Viscosity, Cloud point and Fash Point. *Ind. Crops Prod.*, **43:** 791–797.
30. Moorthi, N. S. V., Franco, P. A. and Ramesh, K. 2015. Application of Design of Experiments and Artificial Neural Network in Optimization of Ultrasonic Energy Assisted Transesterification of Sardinella Longiceps Fish Oil to Biodiesel. *J. Chin. Inst. Eng.*, **38:** 731–741.
31. Muley, P. D. and Boldor, D. 2013. Investigation of Microwave Dielectric Properties of Biodiesel Components. *Bioresour. Tech.*, **127:** 165–174.
32. Oliveira, L. S., Franca, A. S., Camargos, R. R. and Ferraz, V. P. 2008. Coffee Oil as a

[DOR: 20.1001.1.16807073.2019.21.2.14.5]

Potential Feedstock for Biodiesel Production. *Bioresour Tech.*, **99:** 3244-3250.
33. Parkar, P. A., Choudhary, H. A. and Moholkar, **V. S.** 2012. Mechanistic and Kinetic Investigations in Ultrasound Assisted Acid Catalyzed Biodiesel Synthesis. *Chem. Eng. J.*, **187:** 248–260.
34. Rajkovic, K. M., Avramovic, J. M., Milic, P. S., Stamenkovic, O. S. and Veljkovic, **V.** 2013. Optimization of Ultrasound-Assisted Base-Catalyzed Methanolysis of Sunflower Oil using Response Surface and Artificial Neural Network Methodologies. *Chem. Eng. J.*, **215:** 82–89.
35. Ramadhas, A. S., Jayaraj, S., Muraleedharan, C. and Padmakumari, K. 2006. Artificial Neural Networks Used for the Prediction of the Cetane Number of Biodiesel. *Renew. Ener.*, **31:** 2524–2533.
36. Ramos, M. J., Fernández, C. M., Casas, A., Rodríguez, L. and Pérez, Á. 2009. Influence of Fatty Acid Composition of Raw Materials on Biodiesel Properties. *Bioresour Tech.*, **100:** 261-268
37. Rodriguez, R. P., Melo, E. A., Pérez, L. G. and Verhelst, S. 2014. Conversion of By-Products from the Vegetable Oil Industry into Biodiesel and Its Use in Internal Combustion Engines: A Review. *Ener. Braz. J. Chem. Eng.*, **65:** 255–261.
38. Romano, S. D. and Sorichetti, P. A. 2011. *Dielectric Relaxation Spectroscopy in Biodiesel Production and Characterization.* 1st Edition, Springer Verlag, London.
39. Santos, F. F. P., Rodrigues, S. and Fernandes, F. A. N. 2009. Optimization of the Production of Biodiesel from Soybean Oil by Ultrasound Assisted Methanolysis. *Fuel Process. Technol*., **90:** 312–316**.**
40. Sarve, A. N., Varma, M. N. and Sonawane, S. S. 2015. Response Surface Optimization and Artificial Neural Network Modeling of Biodiesel Production from Crude Mahua (*Madhuca indica*) Oil Under Supercritical Ethanol Conditions Using CO_2 as Co-Solvent. *Royal Soci. Chem.*, **5:** 69702–69713.
41. Silva, L. M., Alves Filho, E. G., Simpson, A. J., Monteiro, M. R., Cabral, E., Ifa, D. and Venâncio, T. 2017. DESI-MS Imaging and NMR Spectroscopy to Investigate the Iinfluence of Biodiesel in the Structure of Commercial Rubbers. *Talanta*, **173:** 22-27.
42. Singh, T. N., Kanchan, R., Verma, A. K. and Singh, **S.** 2003. An Intelligent Approach for Prediction of Triaxial Properties using Unconfined Uniaxial Strength. *Min. Eng. J*., **5:** 12–16.
43. Sorichetti, P. A. and Romano, S. D. 2005. Physico-Chemical and Electrical Properties for the Production and Characterization of Biodiesel. *Phys. Chem. Liq.*, **43:** 37–48.
44. Stamenkovic, O. S., Velickovic, A. V., Kostic, M. D., Jokovic, N. M., Rajkovic, K., Milic, P. S. and Veljkovic, V. B. 2015. Optimization of KOH-Catalyzed Methanolysis of Hempseed Oil. *Ener. Conv. Manage.*, **103:** 235–243.
45. Talebian-Kiakalaieh, A. Amin, N. A. S. and Mazaheri, H. 2013. A Review on Novel Processes of Biodiesel Production from Waste Cooking Oil. *Appl. Ener.*, **104:** 683-710.
46. Tan, K., Lee, K. and Mohamed, A. 2011. Potential of Waste Palm Cooking Oil for Catalyst-Free Biodiesel Production. *Energy*, **36:** 2085-2088.
47. Venkatesan, P. and Anitha, S. 2006. Application of a Radial Basis Function Neural Network for Diagnosis of Diabetes Mellitus. *Curr. Sci.*, **91:** 1195–1199.
48. Vicente, G. Martinez, M. and Aracil, J. 2007. Optimisation of Integrated Biodiesel Production. Part I. A Study of the Biodiesel Purity and Yield. *Bioresour Tech.*, **98:** 1724-1733.
49. Yahyaee, R., Ghobadian, B. and Najafi, G. 2013. Waste Fish Oil Biodiesel as a Source of Renewable Fuel in Iran. *Renew. Sust. Ener. Rev.*, **17:** 312–319.
50. Yatish, K. V., Lalithamba, H. S., Suresh, R., Arun, S. B. and Kumar, P. V. 2016. Optimization of Scum Oil Biodiesel Production by using Response Surface Methodology. *Proc. Saf. Env. Prot.*, **102:** 667–672.
51. Yilmaz, I. and Kaynar, O. 2011. Multiple Regression, ANN (RBF, MLP) and ANFIS Models for Prediction of Swell Potential of Clayey Soils. *Exp. Sys. with Appl.*, **38:** 5958–5966.
52. Yilmaz, I. and Yuksek, G**.** 2009. Prediction of the Strength and Elasticity Modulus of Gypsum using Multiple Regression, ANN, and ANFIS Models. *Int. J. Rock Mech. Mining Sci.*, **46:** 803–810.
53. Yin, X., Ma, H., You, Q., Wang, Z. and Chang, J. 2012. Comparison of Four Different Enhancing Methods for Preparing Biodiesel through Transesterification of Sunflower Oil. *Appl. Ener.*, **91:** 320-325.
54. Ying, Y., Shao, P., Jiang, S. and Sun, P. 2009. Artificial Neural Network Analysis of

[DOR: 20.1001.1.16807073.2019.21.2.14.5]

Immobilized Lipase Catalyzed Synthesis of Biodiesel from Rapeseed Soapstock. IFIP *Adv. Info. Commu. Tech.*, **294:** 1239-1249.

55. Zheng, S., Kates, M., Dube, M. A. and McLean, D. D. 2006. Acid-Catalyzed Production of Biodiesel from Waste Frying Oil. *Biom. Bioene.*, **30:** 267-272.

پیش‌بینی و بهینه‌سازی ویژگی‌های بیودیزل ماهی با استفاده از خواص دی‌الکتریک

م. زارعین، م.ه. خوش‌تقاضا، ب. قبادیان، ح. عامری مهابادی

چکیده

هدف از این تحقیق، پیش‌بینی و بهینه‌سازی ویژگی‌های بیودیزل ماهی با استفاده از خواص دی‌الکتریک آن می‌باشد. متغیرهای خواص دی‌الکتریک بیودیزل (έ، ثابت دی‌الکتریک و ε″، فاکتور اتلاف) در فرکانس‌های مایکروویو (۴۳۴، ۹۱۵ و ۲۴۵۰ MHz) به عنوان متغیرهای ورودی مورد استفاده قرار گرفت. ویژگی‌های بیودیزل ماهی، محتوای متیل استر اسید چرب (FAME) و نقطه اشتعال (FP) در سه سطح مختلف زمان واکنش (۳، ۹ و ۲۷ دقیقه) و غلظت کاتالیزور (۱، ۱/۵ و ۲ $\%w/w_{oil}$) به عنوان متغیرهای خروجی مدل در نظر گرفته شد. رگرسیون خطی (LR)، روش‌های شبکه عصبی مصنوعی، پرسپترون چند لایه (MLP) و تابع پایه شعاعی (RBF) و روش سطح پاسخ جهت پیش‌بینی و بهینه‌سازی محتوای FAME و نقطه اشتعال مورد ارزیابی قرار گرفت. مقایسه نتایج نشان داد که RBF بیشترین ضریب تبیین در فرکانس ۲۴۵۰ MHz به میزان ۰/۹۹۹ و ۰/۹۸۸ و پایین‌ترین ریشه میانگین مربعات خطا به میزان ۰/۰۰۹ و ۰/۰۲۳ به ترتیب برای محتوای FAME و نقطه اشتعال داشت. شرایط بهینه با استفاده از RSM برای محتوای FAME به میزان ۸۹/۸۸٪ و نقطه اشتعال به میزان ۱۵۲/۷ $^{\circ}C$ با مطلوبیت ۰/۹۹۸ بدست آمد.

[DOR: 20.1001.1.16807073.2019.21.2.14.5]